Local and long-range order and the influence of applied magnetic field on single-crystalline NiSb_{2}O_{6}

A. B. Christian, C. D. Hunt, and J. J. Neumeier

Phys. Rev. B **96**, 024433 — Published 24 July 2017

DOI: 10.1103/PhysRevB.96.024433

Local and long-range order and the influence of applied magnetic field on single-crystalline $NiSb_2O_6$

A. B. Christian,[1] C. D. Hunt,[2] and J. J. Neumeier[1]

[1]*Department of Physics, Montana State University, Bozeman, Montana 59717-3840, USA*
[2]*Department of Mechanical and Industrial Engineering, Montana State University, Bozeman, MT 59717-3800 USA*

(Dated: June 27, 2017)

The magnetic and thermal properties of single-crystalline $NiSb_2O_6$ are reported. The Ni^{2+} ions exhibit local magnetic order below ∼50 K followed by long-range antiferromagnetic order below $T_N = 6.7$ K. Analysis of the magnetic susceptibility data using the one-dimensional Heisenberg model with spin $\mathbb{S} = 1$ results in a magnetic exchange coupling $J_{||}/k_B \sim 26.0(1)$ K. T_N is observed to either increase or decrease depending upon whether field is applied perpendicular or parallel to the magnetic moment alignment axis. A two-sublattice magnetic structure, with the axis of alignment alternating by 90° between neighboring layers along the crystallographic c axis, is argued to result in two magnetic transition temperatures for certain magnetic field directions, that agrees well with theory. This leads to a highly anisotropic magnetocaloric effect.

PACS numbers: 75.40.-s, 75.30.Gw, 65.40.De, 75.30.Sg

I. INTRODUCTION

Quantum spin chains are model systems of magnetism that demonstrate complex quantum mechanical effects. Thermal and quantum fluctuations play important roles, preventing the development of long-range antiferromagnetic order in the purely one-dimensional (1D) case. In real systems, weak interchain coupling J' can lead to long-range antiferromagnetic order[1] with a Néel temperature T_N that scales approximately with J'. The coupling strength associated with antiferromagnetic order within the chains, $J_{||}$, is stronger than J'. Perturbations by external fields can disrupt the order, resulting in either an increase or decrease[2–5] of T_N, depending upon the direction of the magnetic field with respect to the antiferromagnetic chains.

The shift of T_N with magnetic field can lead to an anisotropic magnetocaloric effect (MCE), which has been reported in some antimony and tantalum oxides.[6] A system exhibiting[6,7] such an anisotropic MCE is $CoSb_2O_6$. It possesses a trirutile crystal structure containing Co-O-O-Co chains within its tetragonal layers, which are parallel to the *a-b* crystallographic planes. Adjacent chains alternate their direction by 90° as they layer along the crystallographic c direction. More specifically, the Co-O-O-Co chains at $z = 0$ point along [110] while those at $z = 1/2$ point along $[1\bar{1}0]$. The associated antiferromagnetic order has magnetic moments on the Co sites at $z = 0$ parallel to [110] and those at $z = 1/2$ parallel to $[1\bar{1}0]$. This structure is called the two-sublattice, or orthogonal, model; it is also known to exist[6] in $NiTa_2O_6$.

The influence of magnetic field on T_N for quantum spin-chain systems has been addressed in some theoretical work.[2–5] The basic idea is the magnetic field can influence the correlation length through its affect on the magnetic correlations.[8] The theory builds on early work by Oguchi,[9] which neglected the affects of anisotropy.[5] The role of magnetic field is to enhance or weaken the anisotropy of the quasi-one-dimension spin-chain system. The theory is restricted to spin systems with a single preferred direction of antiferromagnetic alignment in the ordered state,[5] and can offer only a qualitative understanding of the affect of magnetic field on antiferromagnetism in systems possessing the two-sublattice model.

The present communication deals with a new anisotropic MCE compound, $NiSb_2O_6$. A handful of publications describe[10–13] investigations of polycrystalline $NiSb_2O_6$. This investigation adds to the current level of knowledge through magnetization, specific heat, and thermal expansion measurements of single-crystalline $NiSb_2O_6$. Antiferromagnetic order occurs near 6.7 K, and it possesses the same trirutile crystal structure[14,15] of $CoSb_2O_6$ and $NiTa_2O_6$. The reported magnetic structure is slightly different than the two-sublattice model described above.[16] The best agreement between observed and calculated magnetic reflections was achieved when the magnetic moments are collinear and aligned parallel to [110], forming ferromagnetic and antiferromagnetic chains along the [100] and [010] directions, respectively. The results reported herein are inconsistent with that model, and instead support the two-sublattice model. This is not unexpected, since magnetic structures in these systems have been difficult to uniquely determine via powder neutron diffraction.[7]

II. EXPERIMENT

Polycrystalline samples were prepared from stoichiometric quantities of NiO (99.998%) and Sb_2O_3 (99.999%). The starting materials were mixed, pelletized, and placed in an alumina crucible. The sample was warmed to 1100 °C at 5 °C/min in air, held there for 10 hours, and then cooled to 25 °C at 2 °C/min. One regrinding and re-firing was performed to obtain a pure

phase, which was confirmed, using powder x-ray diffraction, as tetragonal with lattice parameters that agree with prior work.[16]

For the crystal growth, one gram of $NiSb_2O_6$ powder was placed in a quartz ampoule (12 mm o.d, 10 mm i.d, 13.5 cm long) with 100 mg of $TeCl_4$, the Cl-vapor source.[17] The ampoule was evacuated to pressure $P < 1.3 \times 10^{-3}$ mbar, sealed, and placed in a tube furnace. The ampoule was held at 220 °C for one hour, brought to 380 °C at 50 °C/h and held there for one hour. The temperature was then increased to 900 °C at 3 °C/min and a gradient across the ampoule of 4.5 °C/cm was established. It remained under these conditions for 200 h after which it was cooled at 1 °C/min. Crystals formed on the cool side of the ampoule via chemical-vapor transport. The grown crystals were dark green in color and often formed as bicrystals; x-ray diffraction confirmed the crystal structure. Laue x-ray diffraction was used to inspect and orient the crystals which, in some cases, exhibited twinning. The two single crystals used for the measurements reported here exhibited little or no observable twinning; they had masses $m_1 = 10.54$ mg and $m_2 = 4.07$ mg. A single crystal of $ZnSb_2O_6$ was used to represent the lattice contributions to heat capacity and thermal expansion, its preparation was reported previously.[18]

Magnetic susceptibility and heat capacity were measured using a Quantum Design Physical Properties Measurement System. Thermal expansion experiments on sample 1 (with dimensions $a \times b \times c$ equal to $1.47 \times 1.60 \times 1.05$ mm^3) used a fused quartz dilatometer cell,[19] which measures changes in length at a resolution of 0.1 Å. Data near T_N are the average of five measurements, allowing for better temperature resolution. A temperature spacing of 0.1 K was used near the transition and 0.2 K elsewhere. The data for the linear thermal expansion above 10 K were fitted using Chebyshev polynomials[18,19] prior to calculating the thermal expansion coefficient.

III. RESULTS AND ANALYSIS

A. Magnetic measurements

Magnetic susceptibility χ was measured over the temperature range 2 K $< T <$ 300 K. The data, shown in Fig. 1, have been corrected for core diamagnetism ($\chi_{dia} = -112 \times 10^{-6}$ cm^3/mol).[20] Five field directions were measured. Measurements with $H \perp [001]$ (which include $H \| [110]$, $H \| [1\bar{1}0]$, $H \| [100]$, and $H \| [010]$) are identical; only one curve is shown. Analysis over the temperature range 110 K $< T <$ 300 K using the Curie-Weiss equation $\chi = C/(T - \theta) + \chi_0$ revealed minimal differences among the fit parameters for each field direction. From the Curie-Weiss constant C, the paramagnetic moment 3.32(2) μ_B was found. It is close to the value of $3.2\mu_B$ that is typical for Ni^{2+} with spin $\mathbb{S} = 1$, where the orbital angular momentum is quenched.[21] The temperature-independent constant, $\chi_0 = 1.8(6) \times 10^{-4}$ cm^3/mol, is attributed to Van Vleck paramagnetism, and is of similar magnitude to that reported[22,23] for $NiTa_2O_6$. A Curie-Weiss temperature θ = -50(1) K was found.

A transition to long-range order (LRO) is observed as a change in slope of $\chi_{H\|[001]}$ and $\chi_{H\perp[001]}$ at $T_N = 6.7(1)$ K. Plotting the data as $d\chi/dT$ (dashed lines in Fig. 1) highlights the transition. At the lowest temperatures, $\chi_{H\perp[001]} < \chi_{H\|[001]}$, which indicates that the moments are ordered perpendicular to [001]. The fact that the χ data do not tend toward zero as $T \to 0$ for any applied magnetic field direction lying within the a-b plane reveals that antiferromagnetic alignment along a single crystallographic axis within that plane does not occur. Furthermore, the fact that $\chi_{H\|[001]} \approx 2\chi_{H\perp[001]}$ suggests that 1/2 of the moments are perpendicular to H. These two observations are consistent with the two-sublattice model. A slight upturn in $\chi_{H\|[001]}$ below T_N indicates that the magnetic moments are canted by approximately 0.006° along [001].

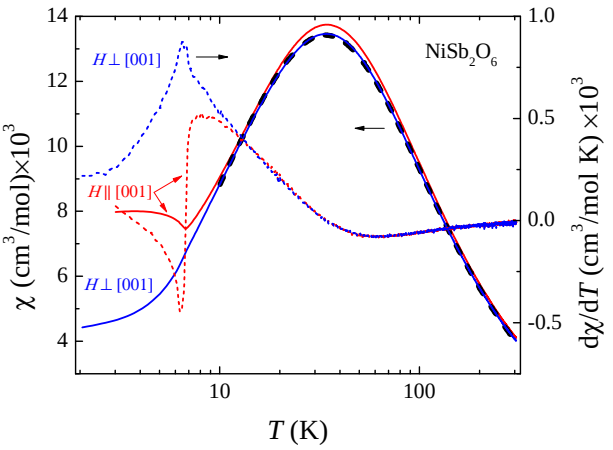

FIG. 1: (color online) Magnetic susceptibility for $NiSb_2O_6$ with $H = 0.2$ T for the indicated field directions. The long-dashed line is a fit to $\chi_{H\perp[001]}$ using the phenomenological expression obtained by Law *et al.*[23] The short-dashed lines are $d\chi/dT$ (right scale), which elucidate the transition at $T_N = 6.7(1)K$.

The $\chi_{H\perp[001]}$ data were fitted over the temperature range 10 K $< T <$ 300 K using an expression[23] based on the one-dimensional Heisenberg model with $\mathbb{S} = 1$. The fit, shown in Fig. 1 with the heavy-dashed line, yields $J_\|/k_B = 26.0(1)$ K, $g = 2.297(3)$, and $\chi_0 = 1.2(1) \times 10^{-4}$ cm^3/mol, that is comparable to the value noted above. Landé g-factors in the neighborhood of 2.25 are typical for Ni^{2+} ions in an octahedral environment.[24] An alternate fit using an Ising model[25] with $\mathbb{S} = 1$ was attempted (not shown) but the result failed to capture the curvature below 40 K.

The influence of magnetic field on T_N is illustrated in the $\chi(T, H)$ data shown in Fig. 2. In the case of $H \| [001]$ (see Fig. 2(a)) T_N moves upward by nearly 1

K at 8 T. The effect is more complex for $H\|[110]$, as shown in Fig. 2(b). Two transitions emerge, which shift away from $T_N(H = 0)$ with increasing field. Similar behavior was observed for $H\|[1\bar{1}0]$. These effects will be discussed below, when the specific heat data are presented. The inset of Fig. 2(a) shows magnetization $M(H)$ at $T = 2$ K. A spin-flop transition at $H \sim 8.1$ T of magnitude $\Delta M \sim 0.04\mu_B$/Ni-ion occurs when the applied field is along either [110] or $[1\bar{1}0]$. No transition is observed for $H < 9$ T along [100], [010], or [001]. This suggests that the antiparallel magnetic moments are ordered along [110] and $[1\bar{1}0]$, consistent with the two-sublattice model.[6]

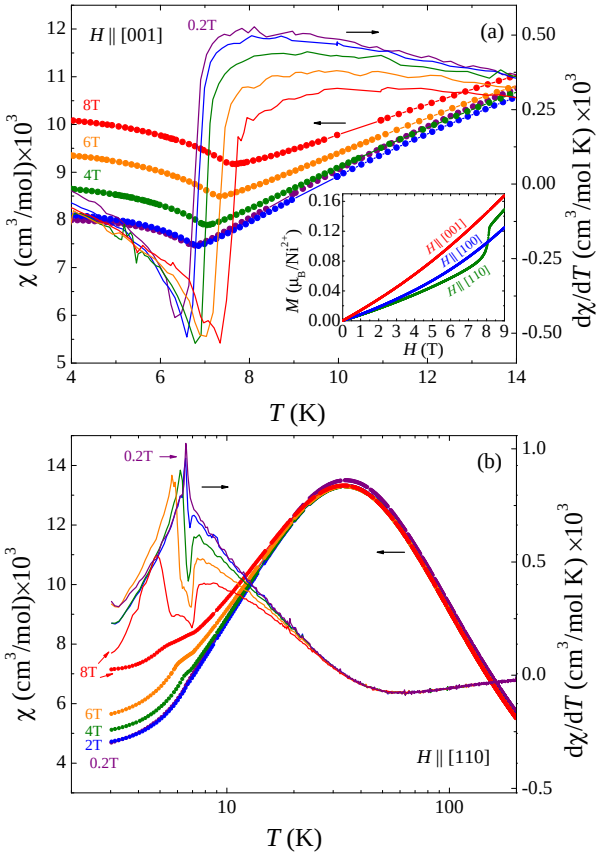

FIG. 2: (color online) Magnetic susceptibility for $NiSb_2O_6$ with (a) $H \parallel [001]$ and (b) $H \parallel [110]$ for applied fields of 0.2, 2, 4, 6, and 8 T. (Inset) Magnetic moment versus applied field at $T = 2$ K. A spin-flop transition is observed at 8.125(5) T for field along either [110] or $[1\bar{1}0]$.

B. Specific Heat Measurements

Specific heat C_P for $NiSb_2O_6$ and $ZnSb_2O_6$ (the nonmagnetic analog compound used for analysis purposes) is shown in the inset of Fig. 3(a). Antiferromagnetic order in $NiSb_2O_6$ is evidenced by a peak at $T_N = 6.7$ K. The $ZnSb_2O_6$ data were subtracted from the $NiSb_2O_6$ data to remove the lattice contribution to C_P. The result scaled by temperature, $\delta C_P/T$ (see Fig. 3(b)), reveals a sharp peak at T_N. The area under the $\delta C_P/T$ curve is the change in entropy ΔS, which reaches 58% of that expected from $R\ln(2\mathbb{S} + 1) = 9.134$ J/mol K, where R is the gas constant (see inset of Fig. 3(b)). Thus, a significant amount of magnetic disorder exists at temperatures well below T_N. Furthermore, the majority reduction of ΔS occurs in the temperature range $T_N < T < 50$ K, illustrating that short-range magnetic order plays an important role in $NiSb_2O_6$. The δC_P data below T_N can be fitted over 2 K $< T <$ 6 K with $\delta C_P = AT^3\exp(-\Delta_m/k_BT)$, which describes antiferromagnetic magnons. The values $A = 17.87(24)$ mJ/mol K^2 and $\Delta_m/k_B = 4.1(1)$ K were obtained (k_B is the Boltzmann constant).[26]

The influence of H on short- and long-range magnetic order was investigated by measuring C_P with H parallel to selected crystallographic directions. In the case of $H\|[001]$, T_N shifts upward similar to the behavior revealed in Fig. 2(a). Furthermore, the peak at T_N is larger, and its width broadens by about 20%. Evaluation of δC_P illustrates that only the peak at T_N shifts, while the broad peak and the magnitude of ΔS are unaffected (not shown). This indicates that $H\|[001]$ has no discernible effect on the overall amount of short-range magnetic order and the increase in peak height at T_N is simply associated with the reduction of entropy over the temperature range in the general vicinity of T_N.

When $H\|[110]$ or $[1\bar{1}0]$, the peak at T_N splits into two peaks, in agreement with the observations in Fig. 2(b). When $H\|[100]$ or [010], no shift in T_N is observed, within our uncertainty. Evaluation of δC_P for these magnetic field directions reveals no discernible affect on ΔS in the region above T_N where short-range order occurs (not shown).

The shift in T_N revealed in $\chi(T, H)$ and $C_P(T, H)$ provide insight into the antiferromagnetic structure in $NiSb_2O_6$. With $H\|[110]$ or $[1\bar{1}0]$, the behavior is identical, with the peak at T_N splitting into two peaks, one moving up in temperature as H is increased, the other moving down. This suggests two magnetic sublattices lying in the a-b plane, one with its magnetic moments perpendicular to H, the other with its magnetic moments parallel to H for these two field directions. This assessment is consistent with the $M(H)$ data shown in the inset of Fig. 2(a) and the $\chi(T, H)$ data of Fig. 2. We therefore postulate that the Ni-O-O-Ni chains at the unit-cell position $z = 0$ point along [110] while those at $z = 1/2$ point along $[1\bar{1}0]$. This antiferromagnetic structure is called the two-sublattice, or orthogonal, model described in the Introduction. It is known to exist in the analogous compounds[6] $CoSb_2O_6$ and $NiTa_2O_6$. This structure differs from the one proposed in a powder neutron diffraction study[16] of $NiSb_2O_6$, where the magnetic moments are parallel to the [110] direction. However, the antiferromagnetic structures of these compounds have proven to be difficult to uniquely determine via neutron powder

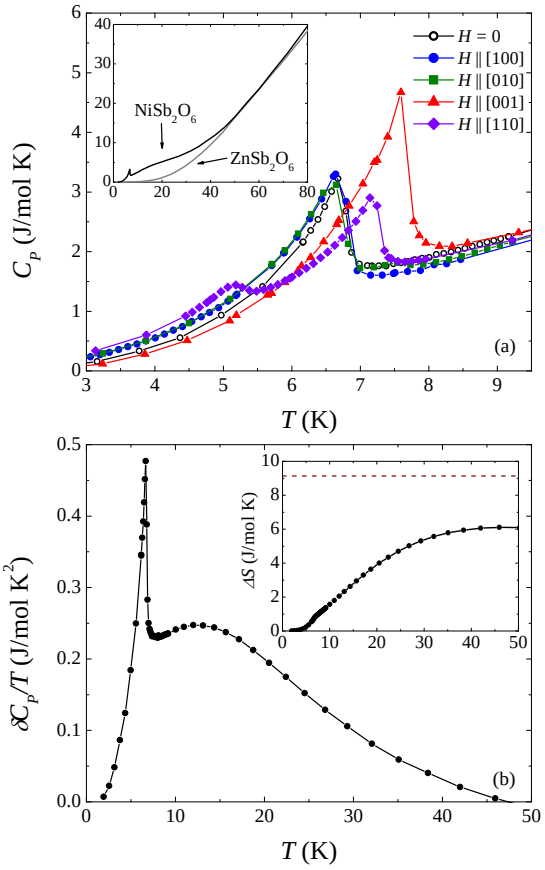

FIG. 3: (color online) (a) Specific heat for $NiSb_2O_6$ at magnetic field $H = 0$ and 8 T for the indicated field directions. The inset shows $NiSb_2O_6$ and $ZnSb_2O_6$ at $H = 0$. (b) Magnetic contribution to the heat capacity δC_P obtained by subtracting C_P of $ZnSb_2O_6$. The area under the curve is the magnetic entropy change, ΔS, plotted in the inset as the solid line along with the maximum theoretical value, $\Delta S = R\ln(2\mathbb{S}+1)$, shown as the dashed line.

diffraction.[6]

C. Comparison of $T_N(H)$ with theory

Purely one dimensional magnetic systems cannot exhibit long-range magnetic order, unless an interchain interaction J' is present.[5] A magnetic field applied to a quasi-1D magnetic system with finite J' affects the correlation length[8] within the magnetic chains, which can influence T_N. Magnetic field also affects the effective anisotropy.[2] For an antiferromagnetic system, the spins prefer to align perpendicular to H. Thus, when H is applied along the hard axis, i.e. perpendicular to the axis along which the spins align, the anisotropy and T_N increase. When H is applied parallel to the easy axis, i.e. parallel to the axis along which the spins align, the anisotropy and T_N decrease. This decrease continues until the spin-flop transition at H_{SF}, above which the magnetic moments align perpendicular to H, changing the hard-axis direction, causing T_N to increase.

Such behavior has been addressed through theory,[2–5,9] which is compared to the data for $NiSb_2O_6$ below. It is important to recognize that the theory is restricted to spin systems with a single preferred direction of antiferromagnetic alignment in the ordered state,[5] and can offer only a qualitative understanding of the affect of magnetic field on antiferromagnetism in a system such as $NiSb_2O_6$, which possesses the two-sublattice model. For the case of magnetic field parallel to the magnetic moments, T_N as a function of H is given by[5]

$$\frac{\Theta}{T_N} = \frac{1}{\pi^3}\int_0^\pi\int_0^\pi\int_0^\pi \frac{\mathrm{d}q_x\mathrm{d}q_y\mathrm{d}q_z}{(H_A/H_E - H^2/2H_E^2) + (1-\cos q_z) + \eta(1-\cos q_x) + \eta(1-\cos q_y)}. \quad (1)$$

This expression was derived using using a two-time temperature-dependent Green function. The terms q_x, q_y, and q_z are the three components of the scalar product of the reciprocal-lattice vector and the position vector. (The reciprocal-lattice vector runs over all the spins in the first Brillouin zone.) When magnetic field is perpendicular to the magnetic moments, T_N as a function of H is given by[5]

$$\frac{\Theta}{T_N} = \frac{1}{\pi^3}\int_0^\pi\int_0^\pi\int_0^\pi \frac{\mathrm{d}q_x\mathrm{d}q_y\mathrm{d}q_z}{2(1+2\eta)\sin^2\phi \pm (K/2J)\cos^2\phi + \cos 2\phi \times [(1-\cos q_z) + \eta(1-\cos q_x) + \eta(1-\cos q_y)]}. \quad (2)$$

In these equations, $\Theta = 4J_\parallel\mathbb{S}(\mathbb{S}+1)/(3k_B)$, H_A is the anisotropy field, H_E is the exchange field, $\eta = J'/J_\parallel$, $\sin\phi = H/(2H_E \pm H_A)$ (note: In both Equation (1) and Equation (2), the + sign is for any field when $H\|[001]$ and the − sign is used when $H > H_{SF}$ with $H\|[110]$ (or $[1\bar{1}0]$).), and K is the uniaxial anisotropy term, which indicates whether a system's behavior is Heisenberg-like (small K) or Ising-like ($K \to \infty$). For an ideal 1D chain, $\eta = 0$.

Since two AFM sublattices exist with magnetic moments perpendicular to c, Equation (1) was used to fit the data for $H\|[110]$ that exhibits the lower T_N values, since it corresponds to H parallel to the magnetic moment alignment axis. An iterative algorithm was employed in fitting the data. The obtained fit parameters are $\eta = 0.00209$, $H_A = 0.2014$ T, and $H_E = 163.9$ T in Equation (1). The value of the exchange coupling was restricted to $J_\|/k_B = 26.0(1)$ K, determined from our one-dimensional Heisenberg model fit to $\chi(T)$. The spin-flop field is approximated[5] by $H_{SF} \approx (2H_AH_E)^{1/2}$. Its measured value was used to constrain H_A and H_E during the fitting procedure.

The values of η, H_E, and H_A determined using the above-described algorithm were then used in the direct calculation of the Néel temperature for the field perpendicular to both chains using Equation (2). If the parameters also produced a satisfactory agreement for the Néel temperature perpendicular to the chains, it was concluded that the obtained values for η, H_E, and H_A were reasonable. If not, the algorithm was set to redo the iterative determination of these parameters using the Néel temperature measured along the axis chain with different initial guesses for the to-be-determined parameters. Once both fits were satisfactory for $H < H_{SF}$, Equation (2) was applied to the $H\|[110]$ data for $H > H_{SF}$.

The obtained uniaxial anisotropy term, $K/k_B = 0.06389$ K, indicates that the system's behavior is Heisenberg-like, with quasi-1D magnetic chains. In contrast, $K/k_B \sim 7$ K determined[27] for $FeTa_2O_6$ (using a different method), was considered large, leading the authors to conclude Ising-like behavior. The small value of η indicates the chains are mostly isolated, as we would expect for low-dimensionality. H_E is larger than expected; it is approximated as the field where parallel alignment of spins occurs by linear extrapolation of $M(H)$ above H_{SF}, yielding $H_E \sim 40$ T. This is about 4 times smaller than the value determined from Equation (1).

D. Thermal Expansion Measurements

The linear thermal expansion $\Delta L/L_{295\,\mathrm{K}}$ along the a- and c-axes for 5 K $< T <$ 350 K is shown in Fig. 5(a), where L is the sample length. Significant anisotropy is observed with $\Delta L/L_{295\,\mathrm{K}}$ along a about 2 times larger than along c over the entire temperature range. Details of the region near T_N are shown for both axes in the insets of Fig. 5(a), where changes in slope at T_N, rather than jumps are evident. This signifies that the phase transition is continuous (i.e. second-order).[28]

The thermal expansion coefficients μ (shown in Fig. 5(b)) were obtained by taking the temperature derivative of the $\Delta L/L_{295\,\mathrm{K}}$ data. The behavior of each axis is similar above 100 K. Below 100 K it is useful to compare μ of $ZnSb_2O_6$ (dashed lines) to μ of $NiSb_2O_6$ (solid lines); both have tetragonal crystal structures. This comparison reveals that the upturns in μ upon cooling can be associated with the presence of short-range magnetic order. As T approaches T_N on cooling, μ approaches zero along c, but remains finite along a. This suggests that the fluctuations associated with short-range magnetic order are most likely confined within the a-b plane.

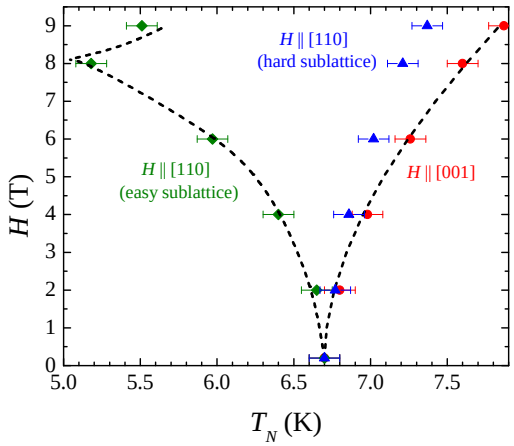

FIG. 4: (color online) Magnetic field versus temperature for $NiSb_2O_6$. $H\|[110]$ results in a decrease of T_N for the chains whose moments are parallel to H, referred to as the *easy sublattice* (green diamonds), and an increase of T_N for the chains whose moments are perpendicular to H, referred to as the *hard sublattice* (blue triangles). $H\|[001]$ (red circles) is perpendicular to the moments of both sets of chains, resulting in an increase of T_N. Dashed black lines show fits using Equations (1) and (2).

The antiferromagnetic phase transition results in peaks of similar magnitude for both axes, as shown in the inset of Fig. 5(b). The data reveal that upon cooling below T_N, an expansion occurs along c and a contraction along a, as one might expect due to the Poisson effect. However, the overall effect on volume is such that the phase transition results in an increase in volume.

In order to analyze the peak near T_N, C_P is written as[29]

$$C_P = T\left(\frac{\partial S}{\partial T}\right)_{T_N} + \nu T\Omega\left(\frac{\partial P}{\partial T}\right)_{T_N}, \qquad (3)$$

where S is the molar entropy, P the pressure, and[16] $\nu = 5.938 \times 10^{-5}$ m^3/mol. The volume thermal expansion coefficient $\Omega = 2\mu_a + \mu_c$, with the subscripts denoting the axes. Equation (3) was determined by considering the phase transition line on the (T,P) plane.[29] The first term in Equation (3) is linear in T, and its subtraction yields $C_P^* \equiv C_P - A - BT$. We define $\lambda = \nu\,(\partial P/\partial T)_{T_N}$. The values A, B, and λ are chosen such that C_P^* and $\lambda\Omega T$ versus T have the best possible overlap. The result is shown in Fig. 6, with $A = 6.1(2)$ J/mol K, $B =$ -0.77(2) J/mol K^2, and $\lambda = 2.85(5) \times 10^5$ J/mol K. The pressure derivative for T_N is obtained from λ as $dT_N/dP = +0.21$

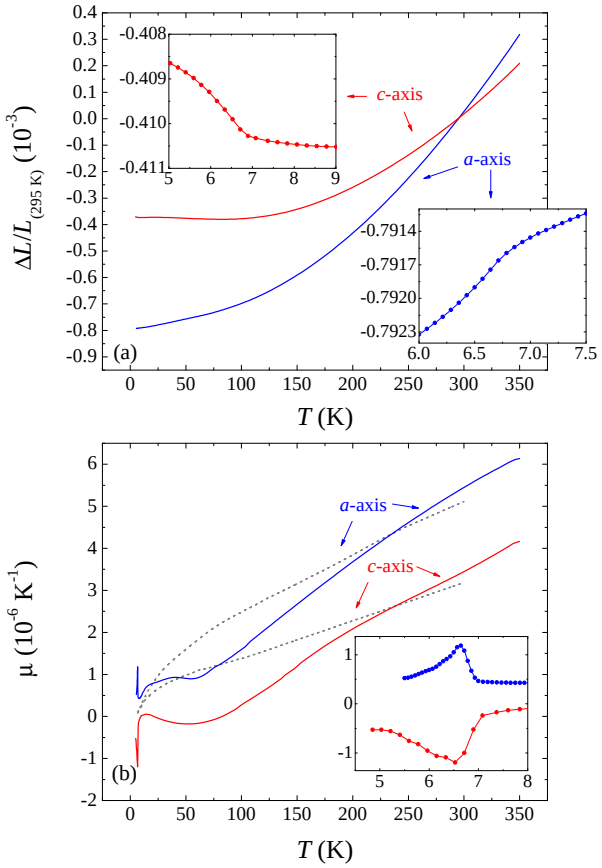

FIG. 5: (color online) (a) Linear thermal expansion $\Delta L/L_{295\,\mathrm{K}}$ for $NiSb_2O_6$. The insets reveal the region near T_N = 6.7 K. (b) Thermal expansion coefficient $\mu = d/dT(\Delta L/L_{295\,\mathrm{K}})$ for $NiSb_2O_6$ (solid lines) and the non-magnetic analog $ZnSb_2O_6$ (dashed lines). The inset details the region near T_N.

K/GPa. The good overlap of the data near T_N suggests that the phase transition is continuous. Note that the deviation of $\lambda\Omega T$ from C_P^* below 6.25 K is associated with the negative thermal expansion along c.

E. Magnetocaloric Effect

The change in entropy associated with the application of magnetic field can be calculated from magnetization $M = \chi H$ through the use of the Maxwell relation

$$\left(\frac{\partial M}{\partial T}\right)_H = \left(\frac{\partial S}{\partial H}\right)_T, \tag{4}$$

which is obtained from the differential of the Helmholtz free energy, under the assumption that the pressure P is constant. Upon integration of Equation (4), we arrive at

$$\Delta S = \int_0^{H_{\max}} \left(\frac{\partial M}{\partial T}\right)_H \mathrm{d}H. \tag{5}$$

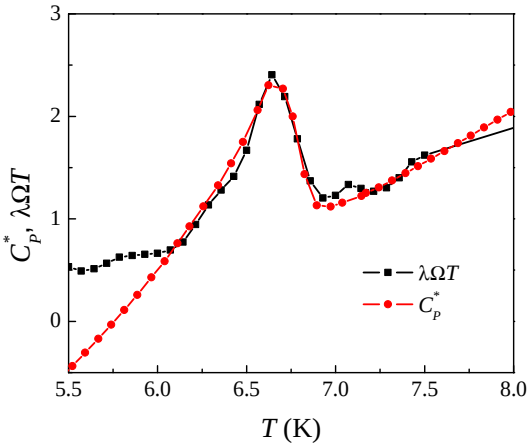

FIG. 6: (color online) Plot of C_P^* and $\lambda\Omega T$ vs temperature illustrating the overlap of heat capacity and volume thermal expansion coefficient data in the vicinity of T_N.

In practice, Equation (5) is used to determine $\Delta S(T, \Delta H)$ by plotting $(\partial M/\partial T)_H$ versus H, and determining the area under the curve. The results are shown in Fig. 7(a) for $H_{\max}$ = 8 T using the filled symbols. The two peaks observed in the data for $H\|[110]$ are associated with the transition temperatures of each sublattice. The change in entropy associated with a change in field tends toward zero at higher temperatures as expected. Notable is the difference in the $|\Delta S(\Delta H)|$ data for the field directions. Rotating the H = 8 T field from $H\|[110]$ or [100] to $H\|[001]$ would lead to $|\Delta S| \sim 0.29$ J/mol K (0.73 J/kg K) near T_N, similar to the value found for $NiTa_2O_6$.[6]

The entropy change can also be calculated from the specific heat using the equation

$$\Delta S(H) = \int_{T_1}^{T_2} \left(\frac{C_P(T,H)}{T}\right) \mathrm{d}T. \tag{6}$$

In this approach, the entropy change associated with the application of magnetic field is determined through ΔS = $\Delta S(H$ = 8 T) - $\Delta S(H$ = 0 T). This method was applied to determine the ΔS values shown by the open symbols in Fig. 7(a). The agreement between the ΔS values obtained using Equation (5) and those obtained using Equation (6) is excellent.

The temperature change associated with a change in magnetic field is calculated using[6]

$$\Delta T = -\int_0^{H_{\max}} \left(\frac{T}{C_P(T,H)}\right)\left(\frac{\partial M}{\partial T}\right)_H \mathrm{d}H. \tag{7}$$

The results are shown in Fig. 7(b) for $H_{\max}$ = 8 T. Note the positive (negative) values of ΔT below T_N for $H\|[001]$ ($H\|[110]$ and $H\|[100]$) in accordance with the shift of the peaks at T_N revealed in Figs. 2 and 3(a).

The MCE can be compared to that of other compounds[30] using the relative cooling power, RCP =

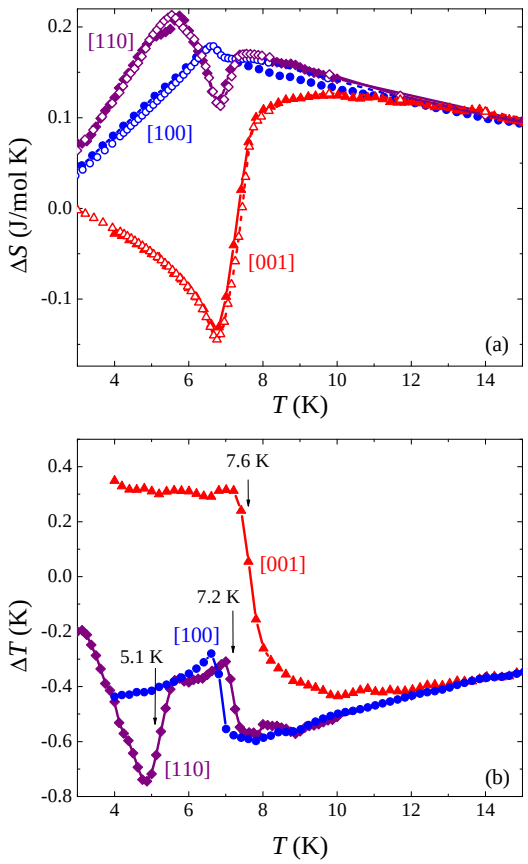

FIG. 7: (color online) (a) Change in magnetic entropy ΔS obtained using Equation (5) (solid symbols) and Equation (6) (open symbols) for a maximum field of $H = 8$ T. (b) Change in temperature ΔT realized through a change in magnetic field of 8 T determined with Equation (7). The Néel temperatures for $H_{\max} \parallel [001]$ (red) and $H_{\max} \parallel [110]$ (purple) are indicated by the arrows.

$-(\Delta S)(\delta T)$, where δT is the width of the ΔS peak at half maximum. The RCP determined from Fig. 7(a) is -2.13 J/mol for $H \parallel [110]$ and -1.57 J/mol and 0.217 J/mol for $H \parallel [001]$ above and below the transition, respectively. These quantities are about two orders of magnitude smaller than gadolinium-based materials.[30]

IV. DISCUSSION AND CONCLUSIONS

Magnetization and thermal measurements on $NiSb_2O_6$ single crystals are reported for the first time. Anisotropy is observed in magnetic susceptibility χ, in-field heat capacity, and thermal expansion data. Three observations reported here are consistent with the two-sublattice model of antiferromagnetism in $NiSb_2O_6$. These are the similarity of behaviors of $\chi(T)$, T_N and $M(H)$ (i.e. the spin-flop transtion) when H is applied along either [110] or $[1\bar{1}0]$. The only possible explanation is that there exists antiparallel alignment of the Ni magnetic moments below T_N that at $z = 0$ point along [110] while those at $z = 1/2$ point along $[1\bar{1}0]$.

The observation that T_N increases when H is parallel to the hard axis seems to be a property of $NiSb_2O_6$ that is unique among this family of transition-metal antimonates and tantalates. In the related compounds, $CoSb_2O_6$ and $NiTa_2O_6$, application of magnetic field along [110] or $[1\bar{1}0]$ also results in a splitting of the peak in heat capacity.[6] However, in those compounds one peak shifts to lower temperature depending upon field strength while the other remains at $T_N(H = 0)$, whereas in $NiSb_2O_6$ *both* peaks shift with applied field. Furthermore, no shift is observed in the related compounds for H parallel to [001], unlike the increase in T_N observed in $NiSb_2O_6$.

An anomalous increase of T_N with applied magnetic field has been observed in other low-dimensional spin systems including $CsNiCl_3$, K_2FeF_5, $Cu_3Mo_2O_9$, and $RbMnF_3$.[2,31–33] Typically, in an AFM when H is parallel to the magnetic moments, T_N is found to decrease to some minimum value, then increase when $H > H_{SF}$. $NiSb_2O_6$ behaves in a similar manner. It has been suggested by Oguchi and Blume[34] that the amount by which T_N increases in response to field is related to the spin entropy; the greater amount remaining at T_N upon cooling, the more the increase of T_N can be seen when an external field is applied. As stated earlier, about 42% of the magnetic entropy remains at T_N for $NiSb_2O_6$. In an 8 T field along [001], T_N increased by about 14%. In contrast, for the similar compound $NiTa_2O_6$, it was observed[6] that about 38% of the total entropy remained at T_N, while an 8 T field along [001] increased T_N by only about 2%. Small variations in the spin entropy can therefore have a significant effect on the in-field long-range order.

The interesting magnetic-field-induced anisotropy observed in specific heat measurements on single-crystalline $NiSb_2O_6$ has potential applications in magnetocalorics. Normally in magnetocaloric systems heat is removed through a multiple-step process that involves applying a magnetic field to a material followed by a reduction of the field either by discharging an electromagnet or removing the material from the field source. If, however, a single crystal of $NiSb_2O_6$ was used as the magnetocaloric material, simply rotating the crystal in a constant magnetic field would result in a change in temperature. While the relatively small RCP cannot compete with gadolinium-based materials for large-scale cooling, $NiSb_2O_6$ may have applications in small-scale systems operating near liquid-helium temperatures.

V. ACKNOWLEDGMENTS

A. C. acknowledges valuable discussions with Y. U. Idzerda. This material is based upon work supported in part by the U. S. Department of Energy (DOE) Grant No. DE-SC0016156.

[1] Z. A., Appl. Phys. A **74**, S1 (2002).

[2] F. Boersma, D. M. Cooper, W. J. M. de Jonge, D. P. E. Dickson, C. E. Johnson, and A. M. C. Tinus, Journal of Physics C: Solid State Physics **15**, 4141 (1982), URL http://stacks.iop.org/0022-3719/15/i=19/a=013.

[3] J. P. A. M. Hijmans, K. Kopinga, F. Boersma, and W. J. M. de Jonge, Phys. Rev. Lett. **40**, 1108 (1978).

[4] F. Boersma, W. J. M. de Jonge, and K. Kopinga, Phys. Rev. B **23**, 186 (1981).

[5] B. B. Singh, H. S. Singh, G. P. Gupta, and K. C. Lal, J. Phys. C: Solid State Physics **18**, 2171 (1985).

[6] A. B. Christian, S. H. Masunaga, A. T. Schye, A. Rebello, J. J. Neumeier, and Y.-K. Yu, Phys. Rev. B **90**, 224423 (2014), URL http://link.aps.org/doi/10.1103/PhysRevB.90.224423.

[7] A. B. Christian, A. Rebello, M. G. Smith, and J. J. Neumeier, Phys. Rev. B **92**, 174425 (2015), URL http://link.aps.org/doi/10.1103/PhysRevB.92.174425.

[8] Villain, J. and Loveluck, J.M., J. Physique Lett. **38**, 77 (1977), URL http://dx.doi.org/10.1051/jphyslet:0197700380207700.

[9] T. Oguchi, Phys. Rev. **133**, A1098 (1964).

[10] A. Nakua and J. Greedan, Journal of Solid State Chemistry **118**, 199 (1995), ISSN 0022-4596, URL http://www.sciencedirect.com/science/article/pii/S002245968571331X.

[11] M. Weil, R. Mathieu, P. Nordblad, and S. A. Ivanov, Crystal Research and Technology **49**, 142 (2014), ISSN 1521-4079, URL http://dx.doi.org/10.1002/crat.201300337.

[12] O. A. Fouad, A. M. Hassan, H. A. El-Wahab, A. M. Eldin, A.-R. M. Naser, and O. A. Wahba, Journal of Alloys and Compounds **537**, 165 (2012), ISSN 0925-8388, URL http://www.sciencedirect.com/science/article/pii/S0925838812008997.

[13] J. Singh, N. Bhardwaj, and S. Uma, Bulletin of Materials Science **36**, 287 (2013), ISSN 0250-4707, URL http://dx.doi.org/10.1007/s12034-013-0454-3.

[14] E. Ramos, M. Veiga, F. Fernández, R. Sáez-Puche, and C. Pico, Journal of Solid State Chemistry **91**, 113 (1991), ISSN 0022-4596, URL http://www.sciencedirect.com/science/article/pii/002245969190063N.

[15] E. Ramos, F. Fernández, A. Jerez, C. Pico, J. Rodriquez-Carvajal, R. Saez-Puche, and M. L. Veiga, Mat. Res. Bull. **27**, 1041 (1992).

[16] H. Ehrenberg, G. Wltschek, J. Rodriguez-Carvajal, and T. Vogt, Journal of Magnetism and Magnetic Materials **184**, 111 (1998), ISSN 0304-8853, URL http://www.sciencedirect.com/science/article/pii/S0304885397011220.

[17] A. V. Prokofiev, F. Ritter, W. Assmus, B. J. Gibson, and R. K. Kremer, Journal of Crystal Growth **247**, 457 (2003), ISSN 0022-0248, URL http://www.sciencedirect.com/science/article/pii/S0022024802020626.

[18] A. Rebello, M. G. Smith, J. J. Neumeier, B. D. White, and Y.-K. Yu, Phys. Rev. B **87**, 224427 (2013), URL http://link.aps.org/doi/10.1103/PhysRevB.87.224427.

[19] J. J. Neumeier, R. K. Bollinger, G. E. Timmins, C. R. Lane, R. D. Krogstad, and J. Macaluso, Review of Scientific Instruments **79**, 033903 (pages 8) (2008), URL http://link.aip.org/link/?RSI/79/033903/1.

[20] R. R. Gupta, *Diamagnetische Suszeptibilität*, vol. 16 of *Landolt-Börnstein, New Series II* (Springer-Verlag, Heidelberg, 1986), ISBN 978-3-540-15953-7.

[21] N. Ashcroft and N. Mermin, *Solid State Physics* (Holt, Rinehart and Winston, 1976).

[22] J. M. Law, H.-J. Koo, M.-H. Whangbo, E. Brücher, V. Pomjakushin, and R. K. Kremer, Phys. Rev. B **89**, 014423 (2014), URL http://link.aps.org/doi/10.1103/PhysRevB.89.014423.

[23] J. M. Law, H. Benner, and R. K. Kremer, Journal of Physics: Condensed Matter **25**, 065601 (2013), URL http://stacks.iop.org/0953-8984/25/i=6/a=065601.

[24] R. L. Carlin and A. J. van Duyneveldt, *Magnetic Properties of Transition Metal Compounds*, vol. 3 (Springer, New York, 1977).

[25] E. G. S. dos Santos, Ph.D. thesis, Université de Grenoble (2012).

[26] S. Blundell, *The Specific Heat of Matter at Low Temperatures* (Imperial College Press, London, 2003).

[27] Y. Muraoka, T. Idogaki, and N. Uryû, J. Phys. Soc. Jpn. **57**, 1758 (1988).

[28] A. B. Pippard, *Classical Thermodynamics* (Cambridge University Press, London, UK, 1961).

[29] J. A. Souza, Y.-K. Yu, J. J. Neumeier, H. Terashita, and R. F. Jardim, Phys. Rev. Lett. **94**, 207209 (2005), URL http://link.aps.org/doi/10.1103/PhysRevLett.94.207209.

[30] K. A. GschneidnerJr, V. K. Pecharsky, and A. O. Tsokol, Reports on Progress in Physics **68**, 1479 (2005), URL http://stacks.iop.org/0034-4885/68/i=6/a=R04.

[31] P. B. Johnson, J. A. Rayne, and S. A. Friedberg, Journal of Applied Physics **50**, 1853 (1979), URL http://scitation.aip.org/content/aip/journal/jap/50/B3/10.1063/1.327143.

[32] T. Hamasaki, H. Kuroe, T. Sekine, M. Akaki, H. Kuwahara, and M. Hase, Journal of Physics: Conference Series **200**, 022013 (2010), URL http://stacks.iop.org/1742-6596/200/i=2/a=022013.

[33] Y. Shapira and N. F. Oliveira, Phys. Rev. B **17**, 4432 (1978), URL http://link.aps.org/doi/10.1103/PhysRevB.17.4432.

[34] T. Oguchi and M. Blume, Journal of the Physical Society of Japan **50**, 2547 (1981), http://dx.doi.org/10.1143/JPSJ.50.2547, URL http://dx.doi.org/10.1143/JPSJ.50.2547.